Received: 25 April 2017 | Accepted: 27 June 2017
DOI: 10.1002/jcp.26068

ORIGINAL RESEARCH ARTICLE

WILEY Journal of Cellular Physiology

Reprogramming mouse embryo fibroblasts to functional islets without genetic manipulation

Bhawna Chandravanshi | **Ramesh Bhonde**

School of Regenerative Medicine, GKVK Post, Allalasandra, Yelahanka, Bangalore, Karnataka, India

Correspondence
Ramesh Bhonde, School of Regenerative Medicine, GKVK Post, Bellary Road, Allalasandra, Yelahanka, Bangalore, Karnataka, India.
Email: rr.bhonde@manipal.edu

Funding information
Manipal University

The constant quest for generation of large number of islets aimed us to explore the differentiation potential of mouse embryo fibroblast cells. Mouse embryo fibroblast cells isolated from 12- to 14-day-old pregnant mice were characterized for their surface markers and tri-lineage differentiation potential. They were subjected to serum-free media containing a cocktail of islet differentiating reagents and analyzed for the expression of pancreatic lineage transcripts. The islet-like cell aggregates (ICAs) was confirmed for their pancreatic properties via immunofluorecence for C-peptide, glucagon, and somatostain. They were positive for CD markers—Sca1, CD44, CD73, and CD90 and negative for hematopoietic markers—CD34 and CD45 at both transcription and translational levels. The transcriptional analysis of the ICAs at different day points exhibited up-regulation of islet markers (*Insulin*, *PDX1*, *HNF3*, *Glucagon*, and *Somatostatin*) and down-regulation of MSC-markers (*Vimentin* and *Nestin*). They positively stained for dithizone, C-peptide, insulin, glucagon, and somatostatin indicating intact insulin producing machinery. In vitro glucose stimulation assay revealed three-fold increase in insulin secretion as compared to basal glucose with insulin content being the same in both the conditions. The preliminary in vivo data on ICA transplantation showed reversal of diabetes in streptozotocin induced diabetic mice. Our results demonstrate for the first time that mouse embryo fibroblast cells contain a population of MSC-like cells which could differentiate into insulin producing cell aggregates. Hence, our study could be extrapolated for isolation of MSC-like cells from human, medically terminated pregnancies to generate ICAs for treating type 1 diabetic patients.

KEYWORDS
C-peptide, dithizone, insulin-like cell aggregates, mesenchymal stem cells, mouse embryo fibroblast

1 | INTRODUCTION

The pursuit for alternative sources of cells for the generation of functional islets is a challenging affair. There is an immense need for the generation of functional islets in bulk for the treatment of type 1 diabetes as progressive destruction of insulin producing cells calls for treatment only via transplantation. Although injecting insulin on a daily basis is crucial for metabolic control, however, the exogenous supply cannot exhibit the physiological control of blood glucose concentrations (Chou, Huang, & Sytwu, 2012). Pancreatic islet transplantation scores better than whole pancreatic organ transplantation therapy due to various side effects leading to thrombosis, pancreatitis, and

peritonitis (White, Shaw, & Sutherland, 2009). However, the challenge still persists due to the dearth of donor pancreatic islets and the lower 5-year insulin independence rate (Berney & Johnson, 2010). Development of tissue replacement therapy compensating an organ donor shortage has become the greatest challenge for the treatment of type 1 diabetes (Sui, Bouwens, & Mfopou, 2013).

The generation of insulin producing islet-like cell aggregates from various sources of stem cell have emerged to be promising for the transplantation therapy. However, the success of stem cell therapy depends on the factors like availability and generation of passable number of islets, preferably an autologous source (Chandra, Phadnis, Nair, & Bhonde, 2009). Mouse embryonic stem (ES) cells have also been widely used for the formation of insulin producing cells (Scroeder, Rolletschek, Blyszczuk, Kania, & Wobus, 2006); however, the differentiation protocol is quite lengthy (33 days). There are many studies reporting the usage of mouse and human embryonic stem cells for generation of pancreatic insulin producing cells (Assady et al., 2001; Baharvand, Jafary, Massumi, & Ashtiani, 2006; Kwon et al., 2005; Segev, Fishman, Ziskind, Shulman, & Itskovitz-Eldor, 2004; Xu et al., 2006). Nonetheless, these sources have various limitations like ethical concern and immunological rejections after transplantation. Next alternative source would be induced pluripotent stems cells (iPS) which has the potential to develop pancreatic endocrine cells (Park et al., 2008; Takahashi et al., 2007). Unfortunately the tumorogenic properties of iPS and ES cells limit their applications in cell based therapies (Kuise et al., 2014).

Adult MSCs could be another option for generation of pancreatic β cells or islets. However, the limited life span of these MSCs is also one of the challenges in generating enormous number of islet. There are various reports on the generation of islets from different non pancreatic sources of human origin (Kadam, Govindasamy, & Bhonde, 2012; Kanafi et al., 2014). Among the diverse source available, mouse embryo fibroblast (MEF) cells are one of the unexplored source for islet generation. The mitotically inactive MEFs are widely used as feeder layers for the prevention of differentiation of mouse embryonic stem (ES) cells (Conner, 2001). MEFs are also reprogrammed for the generation of pluripotent ES cells by inducing the four important transcription factors Oct3/4, Sox2, c-Myc, and Klf4 in ES cell culture conditions (Takahashi & Yamanaka, 2006). There also reports which describes the effective usage of MEF in co-culture conditions for the early development of embryos, the percentage of blastocyst formation was higher when compared to the control (Peters, Spray, & Mendez-Otero, 2016). The effective role of MEFs as feeder layer and in co-culture condition enthusiazed us to determine their differentiation potential. NIH3T3 a mouse embryo fibroblast cell line has been shown to have the potential to differentiate into adipocytes, chondrocytes, and osteocytes and also differentiate into insulin producing cells (Dadheech et al., 2013; Dastagir et al., 2014). However, from the therapeutic point of view using cell lines which are usually transformed and immortalized would be a challenge. We, therefore, wanted to investigate the stemness and differentiation potential of primary MEFs into islet-like cell aggregates.

In the present study, we have illustrated for the first time the stem cell like properties of MEF and their efficiency to differentiate into functional islets, expressing their pancreatic lineage markers and secreting insulin when exposed to glucose.

2 | MATERIALS AND METHODS

2.1 | Isolation and expansion of mouse embryo fibroblasts (MEFs)

MEFs were isolated and propagated using early published protocol (Xu, 2005). Mouse embryos of E13.5-14.5 stage were dissected and all the visceral organs like brain and limbs were removed except for the trunk region. Hereafter, the trunk was immersed in a 50 ml falcon tube containing phosphate buffer saline (PBS) supplemented with penicillin streptomycin and taken to biosafety laminar flow. The tissue chunk was washed thoroughly with PBS containing penstrep. They were further minced into small pieces and then incubated with 2 ml of 0.25% trypsin (Sigma–Aldrich, Darmstadt, Germany) for 10–15 min at 37°C. The trypsin was further neutralized with foetal bovine serum (FBS) (HIMEDIA). They were then spun at 1,000 rpm for 10 min. The supernatant was discarded and the pellet was re-suspended in Alpha—MEM and 10% FBS and seeded in T-25 flask. The cells were then cultured at 37°C in CO_2 incubator with 5% CO_2 (Figure 1a).

2.2 | Population doubling time and growth curve

The population doubling time (PDT) of MEF was assessed. The cells were plated in 60 mm culture dish at a density of 1×10^4 cells/cm^2. The cells were counted until they reached 100% confluency. Population doubling time is calculated using the equation; PDT = culture time/population doubling number (PDN) wherein PDN is calculated according to the formula; PDN = log $N/N0 \times 3.31$, where N is the number of cells harvested at the end of cultivation and $N0$ is the initial seeding density. For the determination of growth curve cells at passages 4 and 12 were seeded at a density of 1×10^4 cells/well in 24 well plates and allowed to reach confluency. The cells were trypsinized every 24 hr and the growth curve was plotted using the average of cell count data at passage 4 as well as passage 12.

2.3 | Isolation and expansion of mouse bone marrow MSCs (m-BM-MSCs)

Mouse bone marrow MSCs (M-BM-MSC) were isolated using a previously published protocol (Truong et al., 2016). In brief, the BM-MSCs were isolated from the femurs of healthy BALB/c mouse. The femurs and tibia were collected in a Petri dish, washed thoroughly with PBS and 70% ethanol in the hood. The muscles were teased completely. Further head of the femur was cut off and marrow was flushed from both the ends by inserting syringe filled with media. The cell suspension was triturated and filtered using a 100 μ strainer. This single cell suspension was then plated on a 35 mm culture dish supplemented with Knockout DMEM (KO DMEM), 10% FBS and

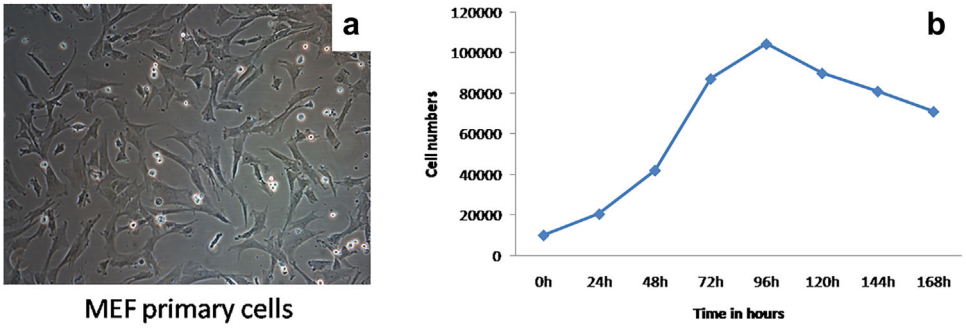

FIGURE 1 Represents the morphology and doubling time of Mouse embryo fibroblast cells (MEF). Subpart (a) depicts the morphology of primary MEF which was isolated in our lab. Whole experiment was conducted on MEF isolated from single donor while subpart (b) represents the exponential growth curve of MEF at passage 4

penstrep and cultured at 37°C in CO_2 incubator with 5% CO_2. Forty-eight hours after initial seeding the floaters were removed and fresh media added. The cells were cultured till passage 3 and further collected for PCR expression of cell surface markers.

2.4 | Characterization of MEF and BM-MSC

2.4.1 | Flowcytometry

Isolated MEFs were first characterized for the expression of exclusive cell surface markers. Flow cytometry was performed for the diverse panels of antibodies such as CD34 (Fluor 4 tagged), CD45, CD44, CD90, Iy6A/E, and Sca1 (PE tagged) (BD Biosciences). Appropriate isotypes were run to determine non-specific fluorescence. MEFs were trypsinized and fixed with 4% paraformaldehyde (PFA) for 30 min at room temperature or overnight at 4°C. The cells were further washed with PBS containing 0.5% bovine serum albumin (BSA) and incubated with specific antibodies dissolved in PBS for an hour on ice. The dilution of antibodies is based on the manufacturer's recommendations. The cells were washed and transferred into fluorescence activated cell sorter (FACS) tubes and acquired on BD FACS Calibur flow. Cell Quest Pro software was used to analyze the data. To confirm

TABLE 1 Represents the list for the sequence of the primers used

Primers list			
Sl No	**Name**	**Forward primer**	**Reverse primer**
I	18S	GTAACCGTTGAACCCCATT	CCATCCAATCGGTAGTAGCG
2	CD 34	TGTGGTTGGTACTGCTGCTC	ACGGTTGGGTAAGTCTGTGG
3	CD 45	AACAACCGACGATGGACTGG	GCCGTGAGTGTGGTGAGGTC
4	CD 44	TGGATCCGAATTAGCTGG	AGCTTTTTCTTCTGCCCAC
5	CD 29	GCCAGGGCTGGTTATACA	TCACAATGGCACACAGGT
6	Sca1	CAATGTAGCAGTTCC	CAGGGGATATAAAGG
7	Nestin	ATACAGGACTCTGCTGGA	AGGACACCAGTAGAACTG
8	Vimentin	AAACTGGAACGGTGAAGGTG	AGAGAAGTGGGGTGGCTTTT
9	HNF3	AAGGGAAATGAGAGGCTGAGTGGA	ATGACAGATCACTGTGGCCCATCT
10	CK-19	AGTTTGAGACAGAACACGCCTTGC	TCAGGCTCTCAATCTGCATCTCCA
11	PDX1	ACTTAACCTAGGCGTCGCACAAGA	GGCATCAGAAGCAGCCTCAAAGTT
12	Glut2	ATTCGCCTGGATGAGTTACG	CAGCAACCATGAACCCAAGG
13	Isl1	ACAAGCGGTGCAAGGACAAGAAAC	ACTGGGTTAGCCTGTAAACCACCA
14	Ngn3	AATCGCATGCACAACCTCAACTCG	AGCGCAGGGTCTCGATCTTTGTAA
15	Pax4	TGTTACAAGACCAGACCACCAGCA	TGCATGCTTCACACTGGTACTCCT
16	NeuroD	ACCTTGCTACTCCAAGACCCAGAA	TTTGCAGAGCGTCTGTACGAAGGA
17	Nkx2.2	TGTGGATTTGAGGGATGTCTGGGT	GGGACAAAGCACCAAGCCAAAGAAT
18	Insulin 2	AGCGTGGCATTGTAGGATCAGTGCT	AGTGGTGGGTCTAGTTGCAGTAGT
19	Glucagon	TGTGAGTTCTTACTTGGAGGGCCA	TGATGAAGTCCCTGGTGGCAAGAT
20	Somatostatin	AGCCCAACCAGACAGAGAATGATG	TCAGAGGTCTGGCTAGGACAACAA

the expressions of cell surface markers, conventional polymerized chain reaction (PCR) was performed. Total RNA extraction of MEF and BM-MSC was carried out using trizol method (Takara) and 1 μg of RNA reversely transcribed using cDNA synthesis kit (Revertaid, Invitrogen) according to the manufacturer's guidance. Conventional PCR was carried out using 2X master mix (Thermo Scientific). The markers were run against 18S (mouse endogenous gene) on 1.8% agarose gel. The primer details are mentioned in Table 1.

2.4.2 | Tri-lineage differentiation

The isolated cells were seeded in 6 well dishes (Corning) for tri-lineage differentiation. The cells were allowed to acquire 80–90% confluency. Further, they were supplemented with chondrogenic (Stempro, A1007101), adipogenic (Stempro, A1007001) and osteogenic (Stempro, A1007201) induction cocktail as per manufacturer's instructions. Cells were replenished with fresh differentiation cocktail media every 4th day for 21 days. The cells were the stained with alcian blue for chondrogenesis, oil o red for adipogenesis and vonkosa for osteogeneis. The images were captured under light microscope (Nikon Eclipse TE 200-S, Chiyoda-Ku, Japan). The tri-lineage differentiation potential of MEF was determined at both passages 4 and 12 in order to determine the efficiency of MEF at even later passage. The undifferentiated cells were also stained along with the differentiated ones to serve as negative control.

2.5 | Differentiation of MEF to ICAs

The generation of ICAs from MEF were performed using our early published protocol (Kadam & Bhonde, 2010). The cells were trypsinized for single cell suspension and were further seeded in serum-free medium containing 1.5% BSA and 1× ITS supplement (5 mg/L of insulin, 5 mg/L of transferrin, and 5 mg/L of selenium). The aggregates were replenished with fresh medium (day 0 medium) containing 0.3 mM Taurine on day 4 and on day 7 the medium was changed with fresh medium (Day 0) supplemented with 100 nM GLP1, 100 μM Nicotinamide, and 3 mM Taurine. The ICAs generated were then stained with dithizone (DTZ) (Figure 3a,b) to determine the presence of β cells.

2.6 | Immunocytochemical characterization

The ICAs generated from MEFs were stained with C-peptide, glucagon, and somatostatin (Abcam) following the routine protocol. They were fixed with 4% PFA for 20 min at room temperature followed by permeabilizing the cell membrane with 0.1% Triton X-100 (Sigma). The ICAs were then washed with PBS and blocked with 5% BSA for 1 hr at room temperature. Further, they were incubated with primary antibody (C-peptide, glucagon, and somatostatin) without washing in 1% BSA overnight at 4°C. Consequently, they were incubated with FITC-conjugated secondary antibody at room temperature for 2 hr. ICAs were then counterstained with 4′,6-diamidino-2-phenylindole (DAPI) for 2–3 min and fluorescent

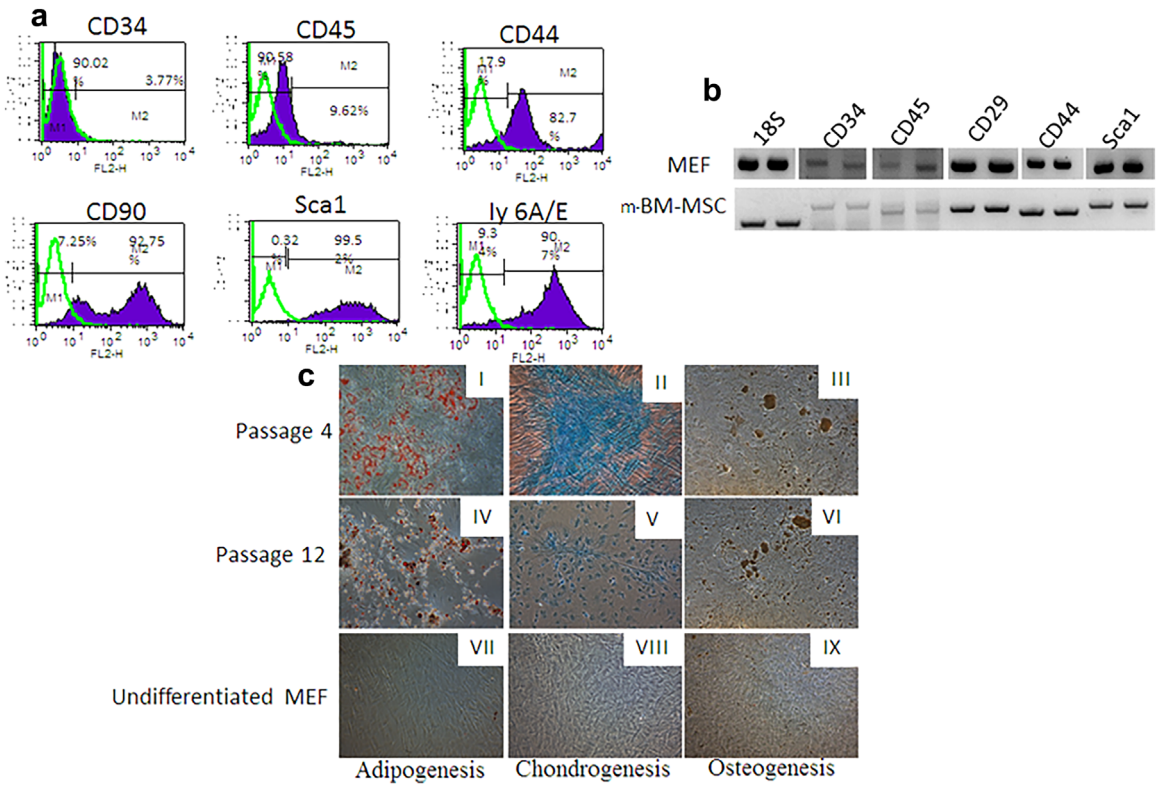

FIGURE 2 Characterization of MEFs. (a and b) Demonstrates the expression of the peculiar cell surface markers via FACS and gene expression. B1 and 2 are the same samples run in duplicates. The tri-lineage differentiation and staining pattern at an early and late passage is demonstrated in subpart (c) along with the staining pattern of undifferentiated cells

images were captured (Nikon). Respective secondary controls were also examined along with the primary incubation to nullify any artefacts.

2.7 | Expression of pancreatic lineage markers

Further, we investigated the expression of pancreatic lineage markers viz; conventional PCR and real time PCR (Rt.PCR). RNA samples were extracted from MEFs and ICAs at different day points, days 3, 7, and 10 using trizol and 1 µg of RNA was reversibly transcribed using cDNA synthesis kit. The samples were analyzed for the expression of pancreatic markers by conventional PCR using 2X master mix (Thermo Scientific). The PCR products were run on 1.8% agarose gel with 18S as the control. The expressions of the markers were further confirmed by Rt.PCR which was carried out using Syber Green PCR master mix (Applied Biosystem) on 7300 Real-Time PCR system (Applied Biosystem). Mouse 18S primers were used to normalize the mRNA values of all the genes studied. The detailed list of the primers is mentioned in Table 1. All the primers were procured from Sigma–Aldrich.

2.8 | Glucose stimulated insulin secretion (GSIS)

The ICAs were further exposed to low (2.5 mM) and high glucose (16.7 mM) concentration to determine their insulin secretion behavior. Insulin secretion assay was performed using and earlier published protocol (Chandravanshi, Datar, & Bhonde, 2015). The ICAs generated from MEF at passages 4 and 12 (4–6) and the primary mouse islets (isolated using our earlier published protocol, Chandravanshi, Dhanushkodi, & Bhonde, 2015) which served as positive control were handpicked and transferred to 24 well plates in quadruplicates. They were washed twice with PBS and glucose starved with 250 µl Kreb's Ringer Hepes Buffer (KRBH) for 1 hr at 37°C in CO_2 incubator. They were washed again and incubated with KRBH buffer containing low (2.5 mmol/L) and high glucose (16.7 mmol/L) for 2 hr. After stimulation the supernatant was collected and stored in −20°C. The ICAs were further lysed for total insulin content in the ICAs. They were lysed with 500 µl of lysis buffer, spun at 10,000 rpm for 10 min and the supernatant was collected and stored in −20°C. Insulin secretion and content was determined by commercially available mouse insulin ELISA kit (Mercodia, AB, Sweden). We also performed the glucose stimulated insulin secretion (GSIS) for MEF cells as a set for negative control. The cells were seeded in 24 well plates (0.02 M cells/well) and post 24 hr of seeding underwent the above-mentioned protocol for glucose stimulation.

Note—lysis buffer composition: 50 mM Tris base, 150 mM sodium chloride, 0.1% Triton X, 1X Protease inhibitor, 10 mM

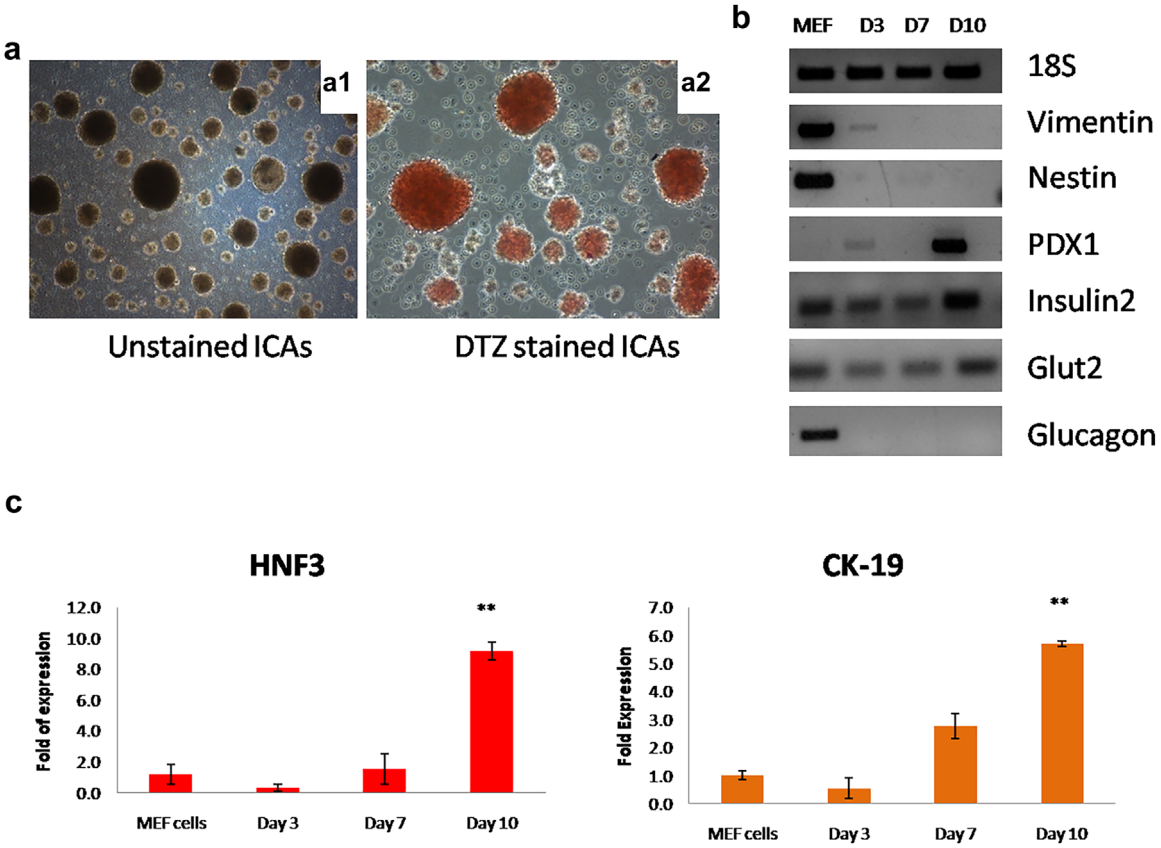

FIGURE 3 Characterization and purity of ICAs derived from MEF. Subpart (a) demonstrates the DTZ staining of the ICAs on the 10th day of differentiation while subpart (b) determines the purity of ICAs at the transcript level with conventional PCR. The ICAs lost their MSC character upon differentiation as evidenced by loss of expression of Vimentin and Nestin at different day points. At the same time the ICAs expressed pancreatic markers like PDX1, Insulin and Glut2. Subpart (c) focuses on the expression of definitive endoderm markers like HNF3 and CK19 via real time PCR. These transcripts were significantly up-regulated in the 10th day ICAs ($p < 0.01$)

sodium fluoride, 0.5 mM sodium molybdate, and 0.5 mM Sodium orthovanadate.

2.9 | Proof of concept under in vivo scenario

A very preliminary work was executed to check the functionality of these ICAs upon transplantation in diabetic mice. Balbc mice ($n = 12$) were made diabetic by single injection of streptozotocin at the dosage of 200 mg/kg body weight. After confirming hyperglycemia these mice 6 of the diabetic mice were injected with 200 ICAs intramuscularly in the thigh muscles while remaining 6 mice were kept as diabetic control. They were observed for a month and were regularly monitored for the glucose level by drawing blood from tail vein. Retro-orbital blood was collected at the end of the experiment for determining the serum insulin level of normal, diabetic, and ICAs-treated mice. The body weight of the mice was monitored and was further plotted in a graph with the average of the normal, diabetic and ICA-treated mice. For all animal work, ethical clearance was obtained from Institutional Animal Ethical Committee.

2.10 | Statistical analysis

All the above-mentioned experiments were performed thrice and the samples were run in quadruplicates ($n = 4$). The data values obtained are represented as mean ± standard deviation (SD). Statistical significance was determined by Students' unpaired t-test and the summary for p values is: <0.05 (*), <0.01 (**), and <0.001 (***), respectively, when compared to control.

3 | RESULTS

3.1 | Population doubling time and growth kinetics

The PDT and the growth curve of MEF indicated their rapid proliferation rate as the PDT was found to be 18 ± 4 hr. Thus, this could be an appropriate source to be scaled up for generating large number of ICAs (Figure 1b).

3.2 | Surface marker expression and multi-potency of MEF

The FACS data revealed that the cells were negative for CD34 (3.77%) and CD45 (9.62%), while positive for CD44 (82.7%), CD90 (92.7%), Sca1 (99.52%), and Iy6A/E (90.7%) (Figure 2a). The PCR result demonstrates that the cells showed very faint band when primed with *CD34* and *CD45* while the band sizes of *CD29*, *CD44*, and *Sca1* were as thick as the endogenous (18S) (Figure 2b). This result was comparable to the expressions of surface markers of m-BM-MSC. The MEFs could

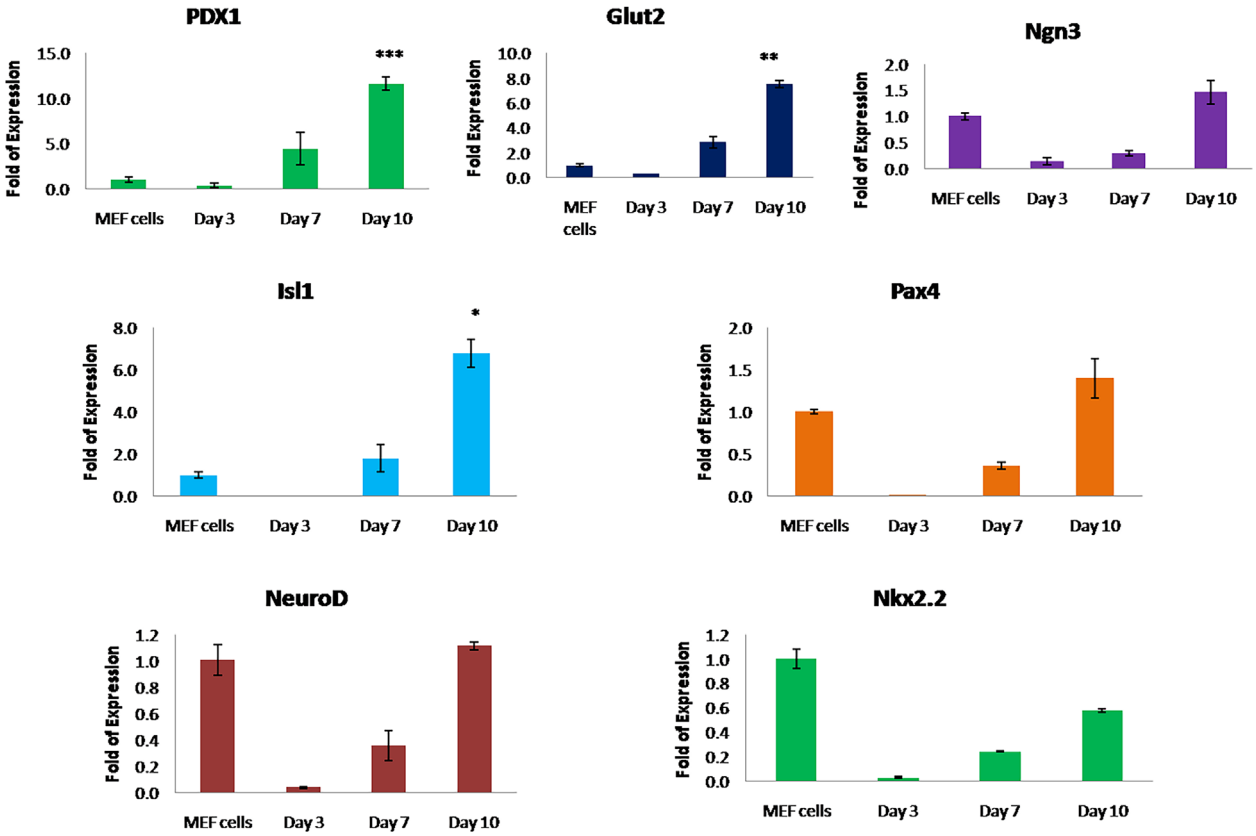

FIGURE 4 Relative expression of Pancreatic endoderm markers. Demonstrates the relative expression of pancreatic endoderm genes such as *PDX1* ($p < 0.001$), *Glut2* ($p < 0.01$), *Ngn3*, *Isl1* ($p < 0.05$), *Pax4*, *NeuroD*, and *NKX2.2*

be differentiated into adipocyte, chondrocyte and osteocyte at both early and late passage (P4 and P12) and stained positive for Oil-O-Red, alcian blue, and vonkossa, respectively (Figure 2c), while the pre-differentiated or the un-differentiated MEFs did not stain positive for Oil-O-Red, alcian blue, and vonkossa.

3.3 | Transcript analysis

The ICAs at different day points were checked for the presence of MSC markers and the pancreatic markers. The markers such as *nestin* and *vimentin* (Figure 3b) were found to be up-regulated only in MEF while they were down-regulated at days 3, 7, and 10 ICAs. On the other hand, the expressions of pancreatic endoderm genes like *PDX1*, *Insulin2*, and *Glut 2* (Figure 3b) gradually increased from days 3 to 7 and finally to day 10 of differentiation, while there expression in MEFs was negligible. To confirm the presence of above pancreatic endodermal genes and few other genes real time PCR was performed. *Insulin 2* (Figure 5) expression up-regulated gradually from day3 to day 5 (twofold) and at day 10 significantly to 18-fold ($p < 0.05$). *PDX1* (Figure 4) showed the similar pattern fivefold increase at day 7 although not significant, while day 10 ICAs showed highly significant ($p < 0.001$) relative expression (10-fold). *Glucagon* (Figure 5) and *Glut 2* (Figure 4) showed similar significant increment in the fold expression (sixfold) ($p < 0.01$) by day 10 ICAs while day 7 ICAs showed twofold increase. Isl1 (Figure 4) and *somatostain* (Figure 5) were also significantly expressed in day 10 ICAs, 7-fold ($p < 0.05$) and 2.5-fold ($p < 0.01$), respectively. Few other pancreatic endodermal markers such as *Ngn3* (Figure 4), *Pax4* (Figure 4), *Nkx2.2* (Figure 4), and *NeuroD* (Figure 4) were not significantly up-regulated in the ICAs while there was significant fold increase in *HNF3* and *CK-19* (Figure 3c) a definitive endodermal marker (10-fold; $p < 0.01$).

3.4 | Immunofluorescence and insulin secretion

The presence of pancreatic markers in ICAs were confirmed by immunofluorescence staining using an early and true pancreatic marker- C-peptide which indicates the presence of insulin producing cells as it is endogenously generated upon cleaving of pro-insulin along with glucagon and somatostatin (Figure 6a–c,g–i,m–o). The ICAs were also analyzed for the respective secondary controls wherein the ICAs were just incubated with secondary antibody without and primary staining (Figure 6d–f,j–l,p–r). Further, the ICAs were stimulated with low and high glucose and it was found that the ICAs generated at both P4 and P12 could respond to glucose concentration. Compared to basal glucose the ICAs significantly enhanced the insulin secretion to 2 ng/ml at P4 ($p < 0.001$) and 1.96 ng/ml at P12 ($p < 0.01$) when stimulated with high glucose (Figure 6s,t). The insulin content, however, remained the same for low and high glucose at different passages (Figure 6u,w). Further, this result was compared with the insulin secretion of primary mouse islets and it was found that mouse islets upon stimulation with high glucose significantly secreted 5.18 ng/ml of insulin ($p < 0.001$) when

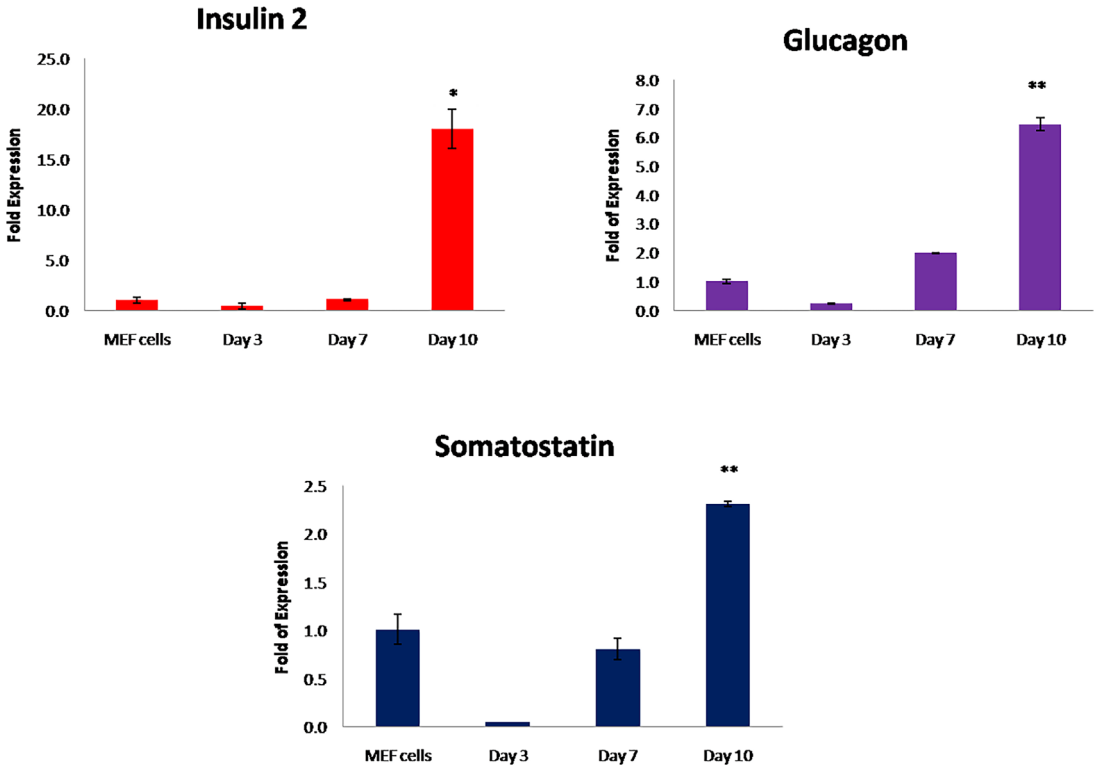

FIGURE 5 Relative expression of Pancreatic hormones. The ICAs showed gradual and significant increase in the relative expression of pancreatic hormones like *Insulin* ($p < 0.05$), *Glucagon* ($p < 0.01$), and *Somatostatin* ($p < 0.01$) as evidenced in figure

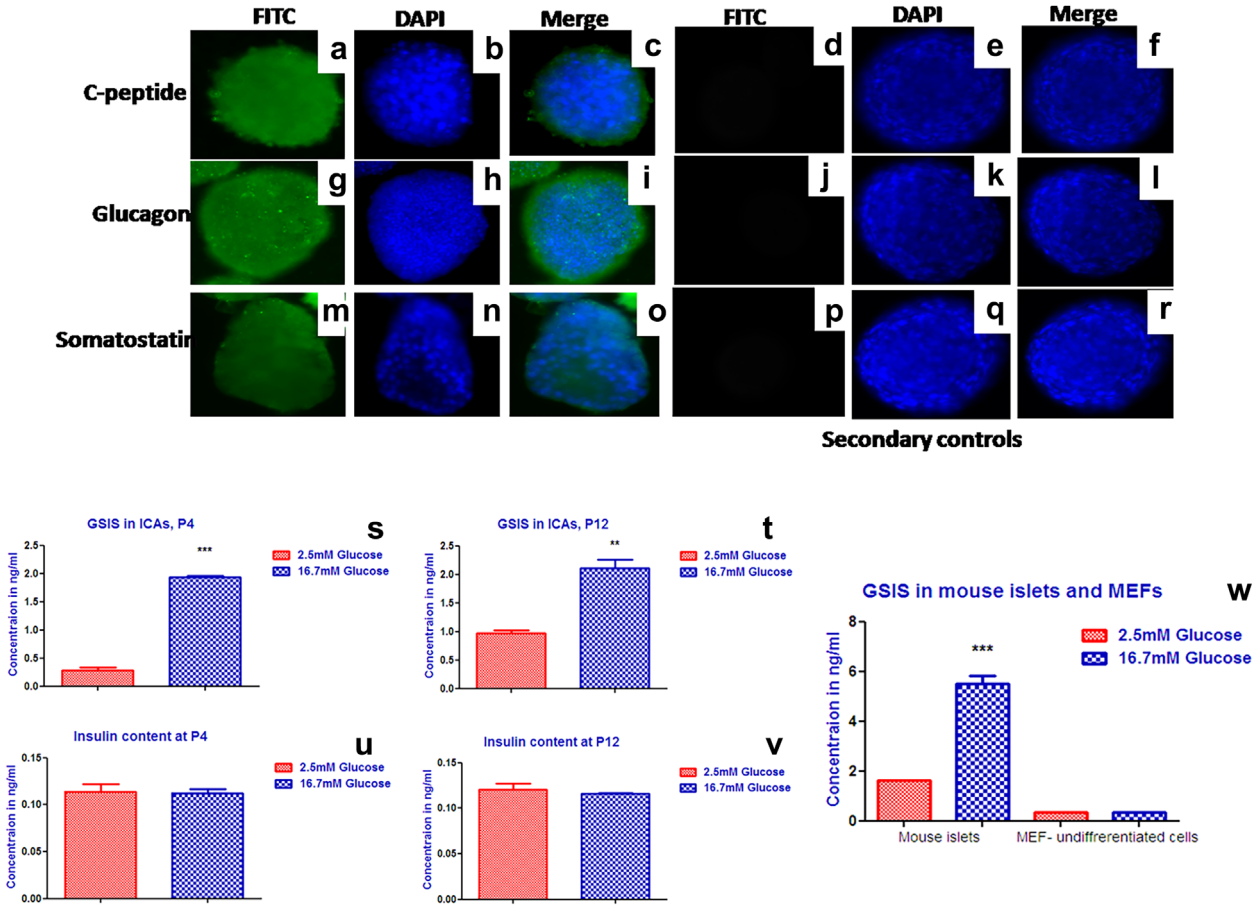

FIGURE 6 Immunofluorescence; insulin secretion and insulin content. Subparts (a–f) describe the immunoflorescence staining of ICAs for C-peptide, glucagon (g–l), and somatostatin (m–r). Subparts (s and t) determines the significant up-regulation of insulin secretion in ICAs generated at P4 ($p < 0.001$) as well as P12 ($p < 0.01$) while subparts (u and v) depict the respective insulin content of the ICAs. Subpart (w) demonstrates the insulin secretion pattern of primary mouse islets ($p < 0.001$) and MEFs

compared to basal glucose (1.63 ng/ml). On the other hand MEFs failed to respond to basal as well as high glucose. Thus this data clearly indicates that the ICAs generated from MEF are functionally active at both early and late passage and the insulin secretion was comparable to that of primary mouse islets.

3.5 | In vivo restoration of normoglycemia and serum insulin

The animals were monitored for a month. Random blood glucose level was checked once in a week and it was found that in non treated diabetic mice the blood glucose level hiked to 500 mg/dl while the treated group showed decreased in hyperglycemia from the 2nd week onward with a constant blood glucose level of 105-110 mg/dl (Figure 7a). We also analyzed the serum insulin level and found that the serum insulin dropped drastically from 0.4 µl U/ml (normal mice) to 0.16 µl U/ml in diabetic mice. However, the serum insulin was restored back to normal 0.3 µl U/ml ($p < 0.01$) (Figure 7b) in ICA-treated mice. The change in body weight was also monitored regularly and at the end of the experiment the ICA-treated mice achieved their normal body weight as compared to the normal mice (Figure 7c). This was just a preliminary work to see whether the system is working or not. Further experiments have to be performed to confirm the study which is our future research plan.

4 | DISCUSSION

MSCs are often described by their plastic adherence, tri-lineage differentiation, explicit marker expression properties, and typical fibroblast-like morphology (Dominici et al., 2006). They can be isolated from various prenatal, neonatal, and adult tissues. Cellular therapies are being investigated due to the immunomodulatory and regenerative properties of MSCs (Hematti, 2012). Despite the fact that various mouse and human MSCs have been directed toward differentiating into insulin producing cells (IPCs), the approach had to be modified due to the extensive protocol and lower efficiencies (Prabakar et al., 2012; Xie et al., 2009). Fibroblast cells on the other hand are also present in almost all the organs which are adherent although not being of endothelium, epithelium, or hematopoietic origin (Haniffa, Collin, Buckley, & Dazzi, 2009). There are several reports which suggest that the fibroblast cells isolated form different organs exhibits similar properties of MSCs. They express the specific

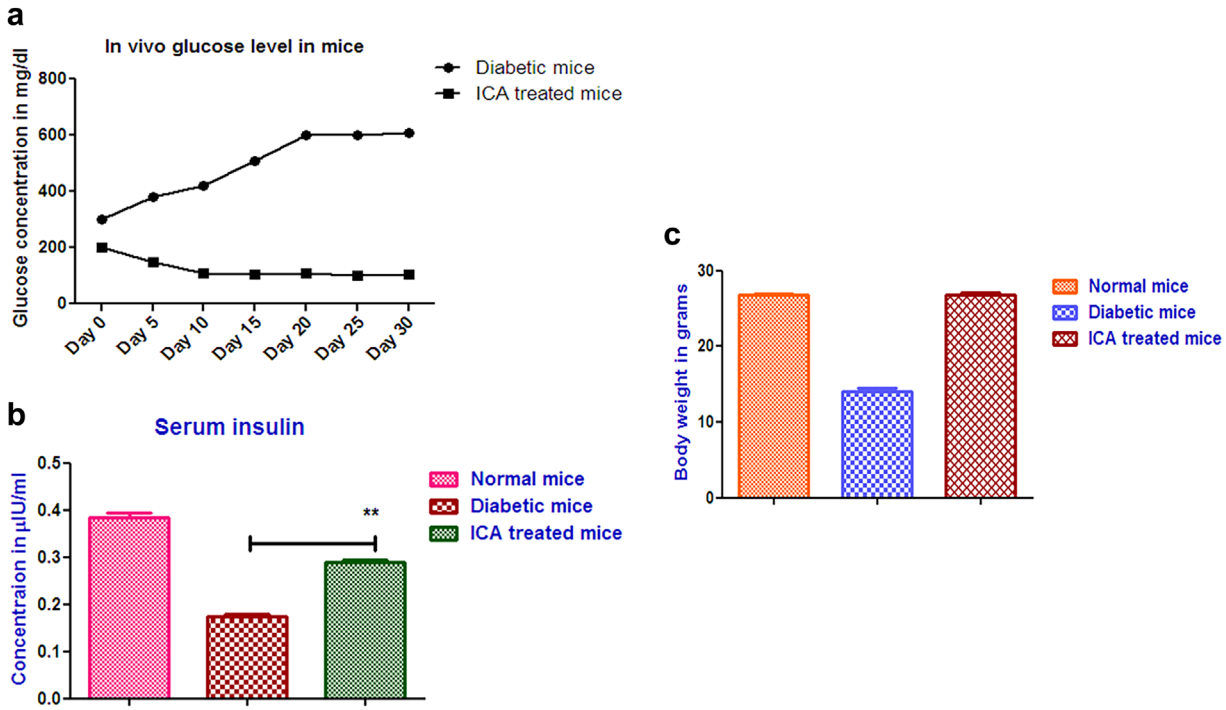

FIGURE 7 Reversal of hyperglycaemia in diabetic mice. Subpart (a) determines the graphical representation of reversal of diabetes in hyperglycaemic mice in time dependent manner when injected with ICAs intramuscularly while subparts (b and c) represent the serum insulin level ($p < 0.01$) and the change in body weight of the mice

marker profiles and can differentiate into fat, bone, and cartilage (Figeac et al., 2015; Kozdon, Fitchett, Rose, Ezra, & Bailly, 2015; Sabatini et al., 2005). Therefore, in the present study, we investigated the stem cell like properties of MEF which are widely used as feeder layers for the maintenance of embryonic stem cells. However, there are reports which describe feeder free human ES culture system (Chunhui et al., 2001). Nonetheless, we found that MEFs exhibit all the benchmark properties of mesenchymal stem cells. It was fascinating to note that these MEFs had robust growth rate and could be maintained in culture till passage 14. The population doubling time was found to be 18–22 h. The exponential growth curve indicated that these MEF proliferated at a higher rate than the MSCs derived from bone marrow of early embryos (Krylova, Musorina, Zenin, Iakovleva, & Polianskaia, 2014).

Flow cytometry and conventional PCR analysis revealed that MEF expressed the panel of typical markers like *CD 29*, *CD44*, *CD90*, *Sca1*, and Iy6A/E articulated in the MSCs, lacking the expression of *CD34* and *CD45* and were comparable to m-BM-MSC which is known to express surface markers and lack hematopoietic markers. They could be differentiated into osteogenic, chondogenic, and adipogenic lineage upon induction with appropriate differentiation cocktail at both early and late passage. The above-mentioned properties of MEF prompted us to differentiate them into ICAs. The extensive growth rate allowed us to generate enormous number of ICAs in a short span, 100 ICAs from 0.1 M cells. The ICAs obtained were all of almost similar sizes ranging between 100 and 130 µ. The ICAs when stained with DTZ which is a zinc chelating agent exhibited brick red color showing there specificity for this stain. DTZ is highly enriched with zinc content which is essential for insulin packaging (Chandravanshi, Datar, et al., 2015). Further we analyzed the expression of MSC transcripts, *nestin* and *vimentin*. Nestin a filament protein is widely expressed in dividing progenitor cells (Lai et al., 2011) and is marker for neural stem cells. Their expression is down-regulated in the differentiated cells and adult stem cells. Vimentin is also an intermediate filament protein which is expressed in mesenchymal cells and is widely used as a marker for cells undergoing epithelial to mesenchymal transition (EMT) (Satelli & Li, 2011). *Nestin* and *Vimentin* were highly up-regulated in the MEF while their expression was down-regulated during the course of differentiation. This confirmed that the cells underwent complete differentiation and were pure population of ICAs. The next phase of our study was to quantify the existence of definitive endodermal markers and pancreatic endoderm markers. The transcripts such as *HNF-3* and *CK-19* (definitive endoderm) were up-regulated in differentiated ICAs. Further, the pancreatic lineage transcripts like *PDX1*, *Glut2*, *Ngn3*, and *Isl1* were up-regulated while *Pax4*, *NeuroD*, and *Nkx2.2* were not expressed during the differentiation path indicating their immature state. One of the earlier studies on human bone marrow MSC revealed that the ICAs generated in vitro from this source were immature, however, they tend to mature when exposed to in vivo microenvironment or niche (Phadnis, Ghaskadbi, Hardikar, & Bhonde, 2010). Our recent study analyzed the transcriptome screening of naive mouse islets and the islet-like clusters (ILCs) derived from pancreatic MSC-like cells suggested that the newly formed ILCs were immature (Gopurappilly & Bhonde, 2015).

Further, we studied the pancreatic endocrine genes by conventional as well as real time PCR. It was observed that the hormones like, *insulin*, *glucagon*, and *somatostatin* were highly up-regulated during the course of differentiation. The up-regulation of all the hormones indicated their functionally active state. Generation of mature ICAs from adult MSCs have already been reported (Chandra et al., 2009; Kanafi et al., 2013). However, the life span of such ICAs would be questionable as they are already mature. On the other hand mouse embryonic fibroblast cells have been successfully reprogrammed earlier with small molecules to develop insulin producing progenitor cells (IPPCs) which expressed all the above-mentioned markers (Li et al., 2014). However, this approach is very extensive as the generation of IPPCs takes 25days and the differentiation cocktail consists of four different small molecules in addition to the normal differentiation cocktail which will be a costly affair. Our differentiation protocol is simplified as it consumes less time and is cost effective. Immunofluorescence of ICAs for C-peptide, glucagon, and somatostatin confirmed the existence of functional insulin secretion machinery. C-peptide, a by-product of insulin determines the amount of insulin being produced in the body (Kumar et al., 2013) and is one of the confirmatory tests for functional assessment of ICAs generated from any source of MSC. The glucose stimulated insulin secretion and total insulin content at P4 and P12 finally confirmed their functional activity. The GSIS results confirmed that MEFs themselves do not secrete insulin upon stimulation; however, their secretion pattern was comparable to primary mouse islets upon differentiation into ICAs. The result was promising as the ICAs responded to glucose. It is well known that MSCs cannot be differentiated into β cells or ICAs if cultured under high glucose (25 mM/L) concentration (Xie et al., 2013), hence we maintained the MEF in alpha MEM (5.5 mM/L) and were differentiated in the same medium. The final confirmation test of ICA is their performance in vivo after transplantation in diabetic mice. Our preliminary in vivo results were quite promising as they exhibited reversal of hyperglycaemia and also restored the serum insulin in STZ diabetic mice comparable to that of normal mice, thus serving a proof of principal for demonstrating in vivo functionality of ICAs. We also found a remarkable improvement in the body weight of the ICA-treated mice. However, a detailed in vivo study has to be performed to translate our in vitro results under in vivo scenario. In our transplantation study, we injected the ICAs intramuscularly in the thigh region to minimize the loss of ICAs upon transplantation. There are reports claiming subcutaneous or intra peritoneal injection or transplantation of islets to be better than in the liver as they lead to severe loss of islets due to low oxygen tension and poor vascularisation (Sakata et al., 2014; Sterkers et al., 2013). Though we have not performed a detailed study on the effect of intramuscular injection; the reversal of hyperglycaemia seen in ICA transplanted mice definitely highlights that the ICAs were viable and functional for a month.

In nutshell, our studies clearly demonstrate for the first time that the mouse embryo fibroblasts are multipotent similar to that of adult mesenchymal cells and have the potential to differentiate into functional ICAs Our study also allows us to anticipate the usage of human aborted foetus of first trimester (medical termination of pregnancy, MTP) as an alternative source for the isolation and expansion of human embryo fibroblasts and differentiating them into ICAs for transplantation in type 1 diabetic patients. Thus our work on generation of ICAs from mouse embryo fibroblasts paves way for ICA generation from human embryo fibroblasts without any genetic manipulation.

ACKNOWLEDGMENTS

Authors wish to thank Dr. TMA Pai Chair grant for providing facilities to carry out the present work and Manipal University for providing PhD scholarship to the first author.

CONFLICTS OF INTEREST

Authors declare no conflicts of interest.

REFERENCES

Assady, S., Maor, G., Amit, M., Itskovitz-Eldor, J., Skorecki, K. L., & Tzukerman, M. (2001). Insulin production by human embryonic stem cells. *Diabetes*, *50*(8), 16917.

Baharvand, H., Jafary, H., Massumi, M., & Ashtiani, S. K. (2006). Generation of insulin-secreting cells from human embryonic stem cells. *Development Growth & Differentiation*, *48*(5), 323–332.

Berney, T., & Johnson, P. R. (2010). Donor pancreata: Evolving approaches to organ allocation for whole pancreas versus islet transplantation. *Transplantation*, *90*(3), 238–243.

Chandra, V., G. S., Phadnis, S., Nair, P. D., & Bhonde, R. R. (2009). Generation of pancreatic hormone-expressing islet-like cell aggregates from murine adipose tissue-derived stem cells. *Stem Cells*, *8*, 1941–1953.

Chandravanshi, B., Datar, S., & Bhonde, R. (2015). Response of chick B islets to insulin secretagogues is comparable to those of human islet equivalents. *Journal of the Pancreas*, *16*, 318–323.

Chandravanshi, B., Dhanushkodi, A., & Bhonde, R. (2015). High recovery of functional islets stored at low and ultralow temperatures. *The Review of Diabetic Studies*, *11*(3–4), 267–278.

Chou, F. C., Huang, S. H., & Sytwu, H. K. (2012). Genetically engineered islets and alternative sources of insulin-producing cells for treating autoimmune diabetes: Quo vadis? *International Journal of Endocrinology*, 2012, 1–9. https://doi.org/10.1155/2012/296485

Chunhui, X., Inokuma, M. S., Denham, J., Golds, K., Kundu, P., Gold, J. D., & Carpenter, M. K. (2001). Feeder-free growth of undifferentiated human embryonic stem cells. *Nature Biotechnology*, *19*, 971–974.

Conner, D. A. (2001). Mouse embryo fibroblast (MEF) feeder cell preparation. *Current Protocols in Molecular Biology*, *23.2*. https://doi.org/10.1002

Dadheech, N., Soni, S., Srivastava, A., Dadheech, S., Gupta, S., Gopurappilly, R., … Gupta, S. (2013). A small molecule swertisin from enicostemma-littorale differentiates NIH3T3 cells into islet-like clusters and restores normoglycemia upon transplantation in diabetic balb/c mice. *Evidence-Based Complementary and Alternative Medicine*, *2013*, 280392. https://doi.org/10.1155/2013/280392

Dastagir, K., Reimers, K., Lazaridis, A., Jahn, S., Maurer, V., Strauß, S., … Vogt, P. M. (2014). Murine embryonic fibroblast cell lines differentiate into three mesenchymal lineages to different extents: New models to investigate differentiation processes. *Cellular Reprogramming*, *16*(4), 241–252. https://doi.org/10.1089/cell.2014.0005

Dominici, M., Le Blanc, K., Mueller, I., Slaper-Cortenbach, I., Marini, F. C., Krause, D. S., … Horwitz, E. M. (2006). Minimal criteria for defining multipotentmesenchymal stromal cells: The International Society for Cellular Therapy position statement. *Cytotherapy*, *8*, 315–317.

Figeac, F., Dagouassat, M., Yorgov, M. M., Gouvello, S. L., Trébeau, C., Sayed, A., … Rodriguez, A. M. (2015). Lung fibroblasts share mesenchymal stem cell features which are altered in chronic obstructive pulmonary disease via the overactivation of the hedgehog signaling pathway. *PLoS ONE*, *10*(3), e0121579.

Gopurappilly, R., & Bhonde, R. (2015). Transcriptional profiling and functional network analyses of islet-like clusters (ILCs) generated from pancreatic stem cells in vitro. *Genomics*, *105*(4), 211–219.

Haniffa, M. A., Collin, M. P., Buckley, C. D., & Dazzi, F. (2009). Mesenchymal stem cells: The fibroblasts' new clothes. *Haematologica*, *94*, 258–263.

Hematti, P. (2012). Mesenchymal stromal cells and fibroblasts: A case of mistaken identity? *Cytotherapy*, *14*, 516–521.

Jasmin, Peters, V. M., Spray, D. C., & Mendez-Otero, R. (2016). Effect of mesenchymal stem cells and mouse embryonic fibroblasts on the development of pre implantation mouse embryos. *In Vitro Cellular & Developmental Biology Animal*, https://doi.org/10.1007/s11626-015-9997-5

Kadam, S. S., & Bhonde, R. R. (2010). Islet neogenesis from the constitutively nestin expressing human umbilical cord matrix derived mesenchymal stem cells. *Islets*, *2*(2), 1–9.

Kadam, S., Govindasamy, V., & Bhonde, R. (2012). Generation of functional islets from human umbilical cord and placenta derived mesenchymal stem cells. *Methods in Molecular Biology*, *879*, 291–313.

Kanafi, M. M., Mamidi, M. K., Sureshbabu, S. K., Shahani, P., Bhawna, C., Warrier, S. R., & Bhonde, R. (2014). Generation of islet-like cell aggregates from human non-pancreatic cancer cell lines. *Biotechnology Letters*, *37*(1), 227–233.

Kanafi, M. M., Rajeshwari, Y. B., Gupta, S., Dadheech, N., Nair, P. D., Gupta, P. K., & Bhonde, R. R. (2013). Transplantation of islet-like cell clusters derived from human dental pulp stem cells restores normoglycemia in diabetic mice. *Cytotherapy*, *10*, 1228–1236.

Kozdon, K., Fitchett, C., Rose, G. E., Ezra, D. G., & Bailly, M. (2015). Mesenchymal stem cell-Like properties of orbital fibroblasts in graves' orbitopathy. *Investigative Ophthalmology and Visual Science*, *56*, 5743–5750.

Krylova, T. A., Musorina, A. S., Zenin, V. V., Iakovleva, T. K., & Polianskaia, G. G. (2014). Comparative characteristics of mesenchymal stem cell lines derived from bone marrow and muscle of limb of early human embryo. *Tsitologiia*, *56*(8), 562–573.

Kuise, T., Noguchi, H., Tazawa, H., Kawai, T., Iwamuro, M., Saitoh, I., … Fujiwara, T. (2014). Establishment of a pancreatic stem cell line from fibroblast-derived induced pluripotent stem cells. *Bio-Medical Engineering*, *13*, 64.

Kumar, A., Nigro, A. L., Gysemans, C., Cai, Q., Esguerra, C., Holte, M. N., … Barajas, M. (2013). Reversal of hyperglycemia by insulin-secreting rat bone marrow- and blastocyst-derived hypoblast stem cell-like cells. *PLoS ONE*, *8*(5), e63491.

Kwon, Y. D., Oh, S. K., Kim, H. S., Ku, S. Y., Kim, S. H., Choi, Y. M., & Moon, S. Y. (2005). Cellular manipulation of human embryonic stem cells by TAT-PDX1 protein transduction. *Molecular Therapy*, *12*(1), 28–32.

Lai, S., Piras, F., Mura, E., Spiga, S., Perra, M. T., Minerba, L., … Sirigu, P. (2011). Nestin and vimentin intermediate filaments expression in cutaneous melanoma. International journal of anatomy and embryology. *Histopathology*, *62*(3), 487–498.

Li, K., Zhu, S., Russ, H. A., Xu, S., Xu, T., Zhang, Y., … Ding, S. (2014). Small molecules facilitate the reprogramming of mouse fibroblasts into pancreatic lineages. *Cell Stem Cell*, *14*(2), 228–236.

Park, I. H., Arora, N., Huo, H., Maherali, N., Ahfeldt, T., Shimamura, A., … Daley, G. Q. (2008). Disease-specific induced pluripotent stem cells. *Cell*, *134*(5), 877–886.

Phadnis, S. M., Ghaskadbi, S. M., Hardikar, A. A., & Bhonde, R. R. (2010). Mesenchymal stem cells derived from bone marrow of diabetic patients portrait unique markers influenced by the diabetic microenvironment. *The Review of Diabetic Studies*, *6*(4), 260–270.

Prabakar, K. R., Dominguez-Bendala, J., Molano, R. D., Pileggi, A., Villate, S., & Ricordi, C. (2012). Generation of glucose-responsive, insulin-producing cells from human umbilical cord blood-derived mesenchymal stem cells. *Cell Transplantation*, *21*(6), 1321–1339.

Sabatini, F., Petecchia, L., Tavian, M., Jodon de Villeroché, V., Rossi, G. A., & Brouty-Boyé, D. (2005). Human bronchial fibroblasts exhibit a mesenchymal stem cell phenotype and multilineage differentiating potentialities. *Laboratory Investigation*, *85*(8), 962–971.

Sakata, N., Aoki, T., Yoshimatsu, G., Tsuchiya, H., Hata, T., Katayose, Y., … Unno, M. (2014). Strategy for clinical setting in intramuscular and subcutaneous islet transplantation. *Diabetes/Metabolism Research and Reviews*, *30*(1), 1–10. https://doi.org/10.1002/dmrr.2463

Satelli, A., & Li, S. (2011). Vimentin in cancer and its potential as a molecular target for cancer therapy. *Cellular and Molecular Life Sciences*, *68*(18), 3033–3046.

Scroeder, I. S., Rolletschek, A., Blyszczuk, P., Kania, G., & Wobus, A. M. (2006). Differentiation of mouse embryonic stem cells to insulin-producing cells. *Nature Protocols*, *1*(2), 495–507.

Segev, H., Fishman, B., Ziskind, A., Shulman, M., & Itskovitz-Eldor, J. (2004). Differentiation of human embryonic stem cells into insulin-producing clusters. *Stem Cells*, *22*(3), 265–274. https://doi.org/10.1634/stemcells.22-3-265

Sterkers, A., Hubert, T., Gmyr, V., Torres, F., Baud, G., Delalleau, N., … Pattou, F. (2013). Islet survival and function following intramuscular auto-transplantation in the mini pig. *American Journal of Transplantation*, *13*(4), 891–898. https://doi.org/10.1111/ajt.12136

Sui, L., Bouwens, L., & Mfopou, J. K. (2013). Signaling pathways during maintenance and definitive endoderm differentiation of embryonic stem cells. *International Journal of Developmental Biology*, *57*(1), 1–12.

Takahashi, K., Tanabe, K., Ohnuki, M., Narita, M., Ichisaka, T., Tomoda, K., & Yamanaka, S. (2007). Induction of pluripotent stem cells from adult human fibroblasts by defined factors. *Cell*, *131*(5), 861–872.

Takahashi, K., & Yamanaka, S. (2006). Induction of pluripotent stem cells from mouse embryonic and adult fibroblast cultures by defined factors. *Cell*, *126*, 663–676.

Truong, N. H., Nguyen, N. H., Le, T. V., Vu, N. B., Huynh, N., Nguyen, T. V., … Pham, P. V. (2016). Comparison of the treatment efficiency of bone marrow-derived mesenchymal stem cell transplantation via tail and portal veins in CCl4-induced mouse liver fibrosis. *Stem Cells International*, *2016*, 5720413.

White, S. A., Shaw, J. A., & Sutherland, D. E. (2009). Pancreas transplantation. *The Lancet*, *373*(9677), 1808–1817.

Xie, H., Wang, Y., Zhang, H., Qi, H., Zhou, H., & Li, F. R. (2013). Role of injured pancreatic extract promotes bone marrow-derived mesenchymal stem cells efficiently differentiates into insulin-producing cells. *PLoS ONE*, *8*(9), e76056.

Xie, Q. P., Huang, H., Xu, B., Dong, X., Gao, S. L., Zhang, B., & Wu, Y. L. (2009). Human bone marrow mesenchymal stem cells differentiate into insulin-producing cells upon microenvironmental manipulation in vitro. *Differentiation*, *77*(5), 483–491. https://doi.org/10.1016/j.diff.2009.01.001

Xu, J. (2005). Preparation, culture, and immortalization of mouse embryonic fibroblasts. *Current Protocols in Molecular Biology*, Chapter 28:Unit 28.1.

Xu, X., Kahan, B., Forgianni, A., Jing, P., Jacobson, L., Browning, V., … Odorico, J. (2006). Endoderm and pancreatic islet lineage differentiation from human embryonic stem cells. *Cloning and Stem Cells*, *8*(2), 96–107.

How to cite this article: Chandravanshi B, Bhonde R. Reprogramming mouse embryo fibroblasts to functional islets without genetic manipulation. *J Cell Physiol*. 2018;233:1627–1637. https://doi.org/10.1002/jcp.26068